doi:10.1093/brain/awaa430 BRAIN 2020: Page 1 of 17 | 1

BRAIN
A JOURNAL OF NEUROLOGY

Central opioid receptors mediate morphine-induced itch and chronic itch via disinhibition

Zilong Wang,[1,†] Changyu Jiang,[1,†] Hongyu Yao,[1] Ouyang Chen,[1,2] Sreya Rahman,[1] Yun Gu,[1] Junli Zhao,[1] Yul Huh[1,2] and Ru-Rong Ji[1,2,3]

[†]These authors contributed equally to this work.

Opioids such as morphine are mainstay treatments for clinical pain conditions. Itch is a common side effect of opioids, particularly as a result of epidural or intrathecal administration. Recent progress has advanced our understanding of itch circuits in the spinal cord. However, the mechanisms underlying opioid-induced itch are not fully understood, although an interaction between μ-opioid receptor (MOR) and gastrin-releasing peptide receptor (GRPR) in spinal GRPR-expressing neurons has been implicated. In this study we investigated the cellular mechanisms of intrathecal opioid-induced itch by conditional deletion of MOR-encoding *Oprm1* in distinct populations of interneurons and sensory neurons. We found that intrathecal injection of the MOR agonists morphine or DAMGO elicited dose-dependent scratching as well as licking and biting, but this pruritus was totally abolished in mice with a specific *Oprm1* deletion in Vgat$^+$ neurons [*Oprm1-Vgat* (*Slc32a1*)]. Loss of MOR in somatostatin$^+$ interneurons and TRPV1$^+$ sensory neurons did not affect morphine-induced itch but impaired morphine-induced antinociception. *In situ* hybridization revealed *Oprm1* expression in 30% of inhibitory and 20% of excitatory interneurons in the spinal dorsal horn. Whole-cell recordings from spinal cord slices showed that DAMGO induced outward currents in 9 of 19 Vgat$^+$ interneurons examined. Morphine also inhibited action potentials in Vgat$^+$ interneurons. Furthermore, morphine suppressed evoked inhibitory postsynaptic currents in postsynaptic Vgat$^-$ excitatory neurons, suggesting a mechanism of disinhibition by MOR agonists. Notably, morphine-elicited itch was suppressed by intrathecal administration of NPY and abolished by spinal ablation of GRPR$^+$ neurons with intrathecal injection of bombesin-saporin, whereas intrathecal GRP-induced itch response remained intact in mice lacking *Oprm1-Vgat*. Intrathecal bombesin-saporin treatment reduced the number of GRPR$^+$ neurons by 97% in the lumber spinal cord and 91% in the cervical spinal cord, without changing the number of *Oprm1*$^+$ neurons. Additionally, chronic itch from DNFB-induced allergic contact dermatitis was decreased by *Oprm1-Vgat* deletion. Finally, naloxone, but not peripherally restricted naloxone methiodide, inhibited chronic itch in the DNFB model and the CTCL model, indicating a contribution of central MOR signalling to chronic itch. Our findings demonstrate that intrathecal morphine elicits itch via acting on MOR on spinal inhibitory interneurons, leading to disinhibition of the spinal itch circuit. Our data have also provided mechanistic insights into the current treatment of chronic itch with opioid receptor antagonist such as naloxone.

1 Center for Translational Pain Medicine, Department of Anesthesiology, Duke University Medical Center, Durham, NC 27710, USA
2 Department of Cell Biology, Duke University Medical Center, Durham, NC 27710, USA
3 Department of Neurobiology, Duke University Medical Center, Durham, NC 27710, USA

Correspondence to: Ru-Rong Ji, PhD
Department of Anesthesiology, Duke University Medical Center
Durham, NC 27710, USA
E-mail: ru-rong.ji@duke.edu

Received March 20, 2020. Revised September 29, 2020. Accepted October 22, 2020.

Correspondence may also be addressed to: Zilong Wang
E-mail: zilong.wang@duke.edu

Keywords: inhibitory interneurons; itch; lymphoma; opioid; spinal cord

Abbreviations: CTCL = cutaneous T-cell lymphoma; DNFB = 1-fluoro-2,4-dinitrobenzene; IPSC = inhibitory postsynaptic current; MOR = μ opioid receptor; MPE = maximum possible effect; SDH = spinal dorsal horn

Introduction

Opioids are mainstay pain treatments in clinical medicine. Most opioid analgesics produce antinociception via the μ-opioid receptor (MOR), which is expressed in both the peripheral and central nervous systems (Ji *et al.*, 1995; Matthes *et al.*, 1996; Corder *et al.*, 2018). MOR mediates beneficial effects of opioid analgesics such as antinociception as well as unwanted side effects such as hyperalgesia, opioid induced constipation, and withdrawal responses. Itch is a notable side effect of opioids, particularly following epidural or intrathecal administration. The incidence of pruritus in patients treated systemically with opioids is ∼2–10%, whereas the incidence of pruritus increases to 30–60% of patients receiving intrathecal opioid treatment. Pregnant women have been observed to be more susceptible to pruritus after spinal opioid administration, with an incidence of 60–100% (Reich and Szepietowski, 2010; Kumar and Singh, 2013).

Recent progress has advanced our understanding of the mechanisms of itch (LaMotte *et al.*, 2014; Ji, 2018; Cevikbas and Lerner, 2019). Distinct populations of primary pruriceptors have been demonstrated to sense itch signals (Liu *et al.*, 2009; Han *et al.*, 2013; Mishra and Hoon, 2013; Qu *et al.*, 2014; Pan *et al.*, 2019). Several neurotransmitters and neuromodulators, as well as the involved neurocircuits in itch transmission have been identified (Sun and Chen, 2007; Sun *et al.*, 2009; Carstens *et al.*, 2010; Mishra and Hoon, 2013; Kardon *et al.*, 2014; LaMotte *et al.*, 2014; Huang *et al.*, 2018). Recently, two populations of inhibitory interneurons expressing Bhlhb5 and NPY in the spinal dorsal horn (SDH) have been implicated in regulating chemical and mechanical itch, respectively (Ross *et al.*, 2010; Bourane *et al.*, 2015; Acton *et al.*, 2019; Pan *et al.*, 2019).

Patients with chronic itch commonly experience high sensitivity to pruritogens, mechanically evoked itch sensations, and spontaneous itch (Ikoma *et al.*, 2006; LaMotte *et al.*, 2014). Opioid receptor antagonists (e.g. naloxone, naltrexone, and nalbuphine) have shown to be effective for chronic itch following dermatitis, uremic pruritus, and anti-PD1 immunotherapy induced itch (Brune *et al.*, 2004; Kwatra *et al.*, 2018; Reszke and Szepietowski, 2018; Serrano *et al.*, 2018; Kremer, 2019; Singh *et al.*, 2019). However, we know little about the molecular mechanisms underlying opioid-induced itch beyond a demonstrated interaction between μ-opioid receptor isoform 1D (MOR1D) and gastrin-releasing peptide receptor (GRPR) (Liu *et al.*, 2011). To tackle this problem, we conditionally knocked out MOR in different populations of itch-modulating neurons, including nociceptive sensory neurons expressing transient receptor potential ion channel subtype V1 (TRPV1), inhibitory neurons ($Vgat^+$), and excitatory interneurons in the spinal cord dorsal horn (SDH) expressing somatostatin (SST^+). We demonstrated that MOR in inhibitory interneurons, but not in excitatory interneurons of the SDH, mediates itch following intrathecal μ-opioid treatment. Furthermore, MOR expression in spinal inhibitory interneurons is essential for driving dermatitis-associated chronic itch.

Materials and methods

Reagents

Morphine sulphate was obtained from WEST-WARD pharmaceuticals. Naloxone methiodide (Cat. N192), naloxone (Cat. 1453005), DAMGO (Cat. E7384) GRP (Cat. G8022), histamine (Cat.H7125), chloroquine (Cat. 1118000), and 1-fluoro-2,4-dinitrobenzene (DNFB) (Cat. D1529), and resiniferatoxin (RTX; Cat. R8756) were obtained from Sigma Aldrich. CTOP (Cat. ab120417) was purchased from Abcam. Bombesin-saporin (Cat. IT-40) and blank-saporin (Cat. IT-21) were purchased from Advanced Targeting Systems.

Animals

Oprm1$^{fl/fl}$ (stock No: 030074), *Vgat*-ires-Cre (stock No: 016962), *Sst*-ires-Cre (stock No: 013044), *Trpv1*-Cre (stock No: 017769), Ai32 (stock No: 024109), and Ai9 tdTomato (stock No: 007909) mice, as well as C57BL/6J wild-type mice (stock No: 000664) and NOD CB-17-Prkdc scid mice (stock No: 001303) were purchased from the Jackson Laboratory and maintained at the Duke University Animal Facility. Young mice (1–2 months of age for both sexes) were used for electrophysiological studies. Adult male and female mice (2–4 months) were used for behavioural and pharmacological studies. Mice were group-housed on a 12-h light/12-h dark cycle at 22 ± 1°C with free access to food and water. All mice were randomized when assorted for animal experiments. Sample sizes were estimated based on our previous studies for similar types of behavioural, biochemical, and electrophysiological assays and analyses (Supplementary Table 1) (Chen *et al.*, 2014; Han *et al.*, 2018; Wang *et al.*, 2020). Two to five mice were housed per cage. The animal studies were approved by Institutional Animal Care and Use Committee (IACUC) of Duke University. Animal experiments were conducted in accordance with the National

Institutes of Health Guide for the Care and Use of Laboratory Animals and ARRIVE guidelines.

Drug injection

For intrathecal injections, lumbar puncture was made by a Hamilton microsyringe (Hamilton) fitted with a 30-G needle between the L5 and L6 spinal levels to deliver reagents (5 µl) into CSF in non-anaesthetized mice (Hylden and Wilcox, 1980). Puncture of the dura was indicated by a reflexive lateral flick of the tail or formation of an 'S' shape by the tail. For intradermal administration, a volume of 50 µl of pruritogen was injected into the skin of the nape with a 30-G needle. For the ablation of GRPR$^+$ neurons, mice were given intrathecal injection of 400 ng bombesin-saporin 10 days before behavioural testing, and an intrathecal injection of 400 ng blank-saporin was included as control (Pan *et al.*, 2019). For the ablation of TRPV1$^+$ neurons or fibres, mice received subcutaneous injections of increasing doses of RTX (30, 70, and 100 µg/kg on Days 1, 2, and 3) (Liu *et al.*, 2010*a*; Berta *et al.*, 2014).

Behavioural assessment for itch response

Mice were shaved on the nape or back under light anaesthesia with isoflurane. Before experiments, mice were habituated in small plastic chambers (14 × 18 × 12 cm) for 2 days. Room temperature and humidity levels remained constant and stable for all experiments. Mice were given intrathecal injections of morphine, DAMGO, or GRP at the lumbar region, or intradermal injections of morphine, histamine, or chloroquine at the nape. After injection, behaviour was video recorded for 30 min using a Sony HDR-CX610 camera. The video was subsequently played back and the number of scratches by each mouse were quantified in a blinded manner. For the intrathecal injection experiments, all the scratches by hind paw were counted. Most scratches were towards the side of the back from the nape to the thoracic segments, as well as a few scratches to the facial area (Supplementary Videos 1 and 2). For the intradermal injection, scratches to the injected region were counted. A scratch was counted when the mouse lifted its hind paw to scratch and then put its paw back to the floor or to its mouth. For the biting and licking behaviour, the duration of a mouse spent on biting or licking the affected hind paw, or the tail was recorded.

DNFB-induced allergic contact dermatitis in neck skin

The allergic contact dermatitis (ACD) model of chronic itch was generated by applying the hapten DNFB onto the back skin as previously described (Liu *et al.*, 2016). DNFB was dissolved in a mixture of acetone and olive oil in a 4:1 ratio. The surface of the abdomen and the nape of neck of each mouse were shaved 1 day before sensitization. On Day 0, mice were sensitized with 50 µl of 0.5% DNFB solution by topical application to a 2 cm^2 area of shaved abdomen skin. On Days 5, 7, 9, and 11 mice were challenged with 30 µl 0.25% DNFB solution painted onto the nape of neck, with 1-h videos taken on Days 6, 8, 10, and 12. Spontaneous scratching was observed for each 1 h recording.

Cutaneous T-cell lymphoma model

The cutaneous T-cell lymphoma (CTCL) model was established in a similar method as our previous study (Han *et al.*, 2018). Briefly, a CD4$^+$ MyLa cell line was purchased from Sigma (Cat. 95051032). The cell line was established from a plaque biopsy of an 82-year-old male with mycosis fungoides stage II by inclusion of IL-2 and IL-4 in the culture medium. CTCL was generated by intradermal injection of CD4$^+$ MyLa cells (1 × 10^5 cells/µl, 100 µl) on the nape of the neck in immune-deficient mice (NOD.CB17-Prkdcscid, 8–10 weeks old, female and male). Itch behaviour was tested 20–30 days after MyLa cell inoculation and the videos were analysed (1 h per analysis).

Tail-flick test

All animals were habituated to the testing environment for at least 2 days before baseline testing. Tail-flick testing was performed as described in a previous report (Wang *et al.*, 2020). Briefly, mice were gently held by hand with a terry glove with tail exposed. The distal 3 cm end of the tail was immersed into a 50°C hot water bath. The tail-flick latency was measured as the time required for the mouse to flick or remove its tail from the water, with a maximum cut-off value of 15 s to prevent thermal injury. Tail-flick latency was determined both before and after drug injection. Data are expressed as the maximum possible effect (MPE) where MPE (%) = 100 × [(post drug response − baseline response)/(cut-off response − baseline response)].

Hotplate test

All animals were habituated to the testing environment for at least 2 days before baseline testing. Hotplate testing was conducted following tail-flick testing. Mice were placed on the hotplate apparatus set at 53°C, and the reaction time was scored when the animal began to exhibit signs of pain avoidance such as jumping or paw licking. A maximum cut-off value of 40 s was set to avoid thermal injury.

In situ hybridization

Animals were deeply anaesthetized with isoflurane and transcardiac perfusion was performed with PBS, followed by 4% paraformaldehyde. After the perfusion, spinal cords were removed and post-fixed in 4% paraformaldehyde overnight at 4°C. The tissues were then cryopreserved in 20% sucrose in PBS for 1 day followed by 30% sucrose in PBS for 1 day. Spinal cord sections (20 µm) were cut using a cryostat. *In situ* hybridization was performed using the RNAscope® system (Advanced Cell Diagnostics) following the manufacturer's protocol and our previous report (Chen *et al.*, 2017; Wang *et al.*, 2020). Pretreatment consisted of dehydration, followed by incubation with hydrogen peroxide and protease IV at room temperature. The Multiplex Fluorescent Kit v2 protocol was followed using commercial probes for MOR (Mm-*Oprm1*-C3, Cat. 315841-C3), VGLUT2 (Mm-*Slc17a6*, Cat.319171-C2), NPY (Mm-*Npy*, Cat.313321-C2), NPY1R (Mm-*Npy1r*, Cat. 427021), PDYN

(Mm-*Pdyn*, Cat. 318771), GRP (Mm-*Grp*, Cat. 317961-C2), and GRPR (Mm-*Grpr*, Cat. 317871). Fluorescein Evaluation Kit from PerkinElmer (NEL760001KT) was used for the fluorescence signals. *In situ* hybridization images were captured by Zeiss 880 inverted confocal microscopy. For quantification purposes, all images acquired with the same settings, two to three sections from each animal were selected, and a total of three or four animals for each group were included for data analysis. Visualized cells with more than five puncta per cell were classified as positive neurons.

Spinal cord slice preparation and patch-clamp recordings

Mice were anaesthetized with urethane (1.5–2.0 g/kg, intraperitoneally), the lumbosacral spinal cord was quickly dissected, and the tissue was placed in ice-cold dissection solution (in mM: sucrose 240, $NaHCO_3$ 25, KCl 2.5, NaH_2PO_4 1.25, $CaCl_2$ 0.5 and $MgCl_2$ 3.5), equilibrated with 95% O_2 and 5% CO_2. Mice were sacrificed by decapitation following spinal extraction under anaesthesia. Transverse spinal slices (300–400 μm) were cut using a vibrating microslicer (VT1200s Leica). The slices were incubated at 32°C for 1 h in artificial CSF (in mM: NaCl 126, KCl 3, $MgCl_2$ 1.3, $CaCl_2$ 2.5, $NaHCO_3$ 26, NaH_2PO_4 1.25 and glucose 11), equilibrated with 95% O_2 and 5% CO_2. The slices were then placed in a recording chamber and perfused at a flow rate of 2–4 ml/min with ACSF which was saturated with 95% O_2 and 5% CO_2 and maintained at room temperature (Jiang *et al.*, 2014). Lamina II neurons in lumbar segments were identified as a translucent band under a microscope (BX51WIF; Olympus) with light transmitted from below. *Vgat*-Cre; Ai9 mice were used for the recordings of opioid-induced currents or action potentials. $Vgat^+$ neurons were identified by observed fluorescence.

Whole-cell voltage-clamp recordings were made from lamina II neurons by using patch-pipettes fabricated from thin-walled, fibre-filled capillaries. The patch-pipette solution used to record opioid-induced currents or action potentials contained (in mM): K-gluconate 135, KCl 5, $CaCl_2$ 0.5, $MgCl_2$ 2, EGTA 5, HEPES 5, Mg-ATP 5 (pH 7.3). DAMGO-induced currents were recorded at a holding potential of –70 mV in voltage clamp mode. Action potentials were recorded in current clamp mode. To record light-evoked inhibitory postsynaptic currents (IPSCs), the patch-pipette solution contained (in mM) (Gao *et al.*, 2018): Cs_2SO_4 110, $CaCl_2$ 0.5, $MgCl_2$ 2, EGTA 5, HEPES 5, Mg-ATP 5, tetraethylammonium (TEA)-Cl 5 (pH 7.3). For optogenetic activation of inhibitory interneurons, *Vgat*-Cre; Ai32 mice were used. Blue light illumination (0.1 s) was delivered through a 40× water-immersion microscope (BX51WIF; Olympus) objective to initiate a light-evoked response. The light-evoked IPSCs were recorded in the presence of AP-V (50 μM) and CNQX (2 μM) at a holding potential of 0 mV in voltage clamp mode. The patch-pipettes had a resistance of 8–10 MΩ. Signals were acquired using an Axopatch 700B amplifier. The data were analysed with pCLAMP 10.3 software. Currents were measured by Clampfit. Numerical data are given as the mean ± standard error of the mean (SEM). In all cases, *n* refers to the number of the neurons studied. All drugs were bath applied by gravity perfusion via a three-way stopcock without any change to the perfusion rate.

Statistical analyses

All data are expressed as mean ± SEM as indicated in the figure legends. Statistical analyses were completed with Prism GraphPad 6.1. Data were analysed using two-tailed Student's *t*-test (two groups), one-way ANOVA, and two-way ANOVA. The criterion for statistical significance was $P < 0.05$.

Data availability

Original data are available upon request.

Results

Intrathecal opioids induced acute itch via MOR expressed by inhibitory interneurons

We first tested intrathecally injected morphine-induced itch response in wild-type mice. Intrathecal morphine elicited dose-dependent scratch behaviour in wild-type mice (Fig. 1A, $P = 0.0089$). The dose of intrathecal morphine to elicit maximal scratches was 0.3 nmol. For comparison, the higher dose morphine (2 nmol, intrathecal) induced less itch due to possible motor inhibition. Over the time course of treatment, morphine-induced itch responses mainly occurred in the first 30 min after injection. We did not find the sex differences of intrathecal morphine-induced itch between males and females (Supplementary Fig. 1A, $P = 0.5880$). Intrathecal morphine-induced itch was significantly blocked under pretreatment with the MOR selective antagonist, CTOP, which suggests that morphine-induced itch response is mediated by MOR (Fig. 1B, $P = 0.0153$). Next, we examined whether morphine-induced itch is mediated by excitatory or inhibitory neurons in the spinal cord. To this end, we used *Vgat-Cre* or *Sst-Cre* mice crossed with $Oprm1^{fl/fl}$ mice to conditionally knockout MOR on inhibitory or excitatory interneurons (Chamessian *et al.*, 2018; Duan *et al.*, 2018; Huang *et al.*, 2018) in the spinal cord, respectively. Strikingly, conditional deletion of *Oprm1* on inhibitory interneurons completely abolished morphine-induced itch (Fig. 1C, $P = 0.0001$). Biting and licking towards hind paw or the tail after intrathecal morphine injection may reflect itch response to the hindquarters (LaMotte *et al.*, 2011; Qu *et al.*, 2014). Conditional deletion of *Oprm1* on inhibitory interneurons significantly reduced the morphine-induced biting and licking response (Fig. 1D, $P < 0.0001$). This conditional deletion did not change the baseline spontaneous itch (Supplementary Fig. 1B, $P = 0.1166$) or mechanical itch evoked by a 0.7 mN von Frey hair (Supplementary Fig. 1C, $P = 0.7078$). In sharp contrast, conditional deletion of *Oprm1* on excitatory interneurons did not affect morphine-induced itch behaviour (Fig. 1E and F, $P = 0.3653$ and $P = 0.6824$, respectively). These results indicate that intrathecal morphine acts on MOR on inhibitory interneurons to evoke itch response. To confirm the specific involvement of

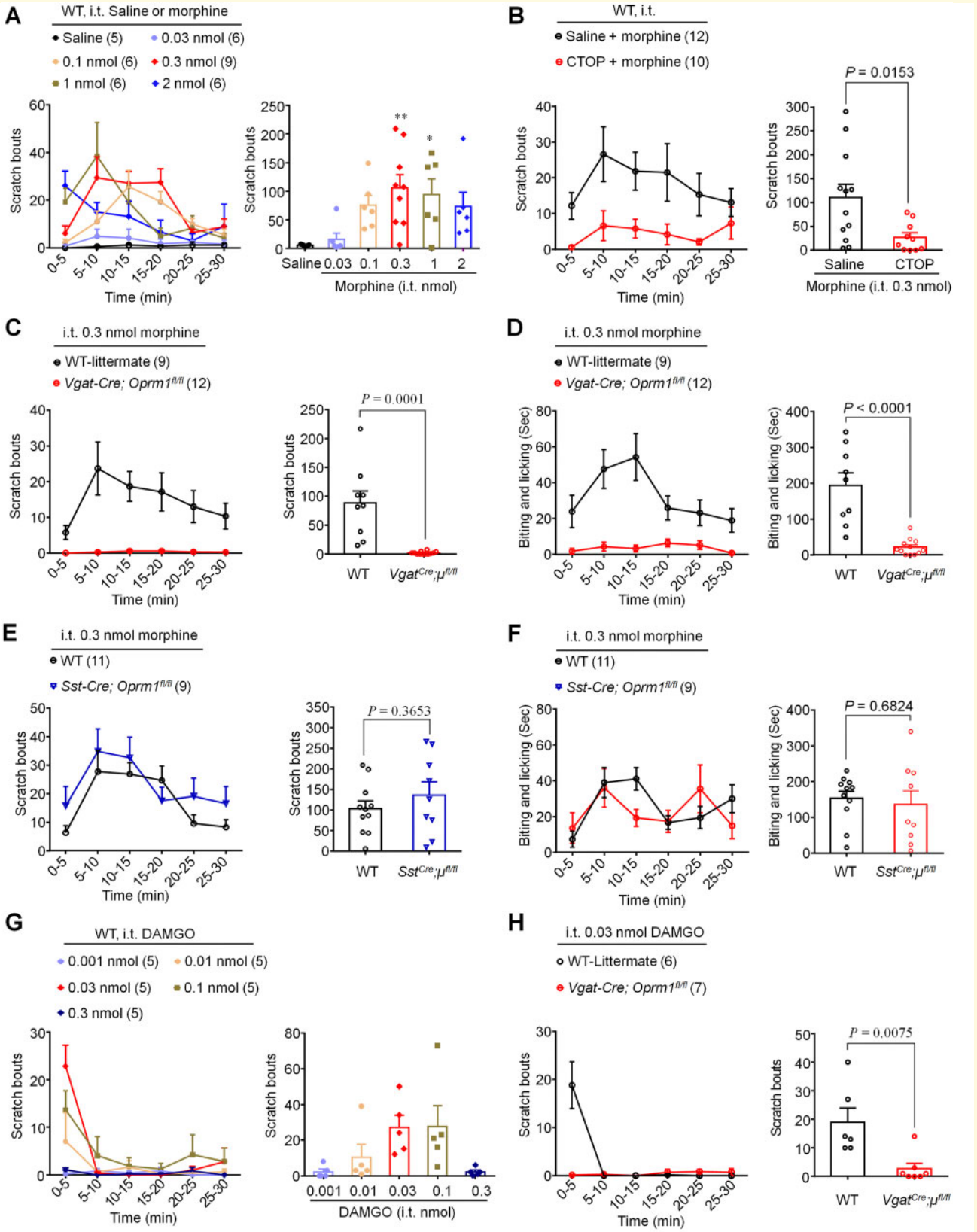

Figure 1 Intrathecal morphine-induced itch requires MOR in spinal inhibitory interneurons. (**A**) Time course (*left*) and total scratch bouts (*right*) within 30 min after intrathecal (i.t.) injection of different doses of morphine in wild-type mice. **P* = 0.0392, ***P* = 0.0086, One-way ANOVA test, followed by Dunnett's *post hoc* test. (**B**) Pretreatments with MOR selective antagonist CTOP (0.15 pmol, i.t.) blocked the morphine (0.03 nmol, i.t.) induced itch response. *P* = 0.0153, two-tailed Student's *t*-test. (**C**) Intrathecal morphine-induced scratches were totally abolished in *Vgat-Cre*; *Oprm1*$^{fl/fl}$ mice. *P* = 0.0001 versus Cre-negative littermates, two-tailed Student's *t*-test. (**D**) Intrathecal morphine-induced biting and

(continued)

MOR in this process, we tested scratching behaviour induced by DAMGO, a MOR-selective agonist. Intrathecal DAMGO induced scratching in a bell-shaped dose response curve, and pruritus mainly occurred in the first 5 min (Fig. 1G). Like morphine, intrathecal DAMGO-induced itch was completely abolished in mice with conditional knockout of MOR on inhibitory interneurons (Fig. 1H, $P = 0.0075$).

Intrathecally injected morphine can act on MOR on dorsal root ganglion afferent terminals and spinal cord neurons. To define the roles of peripheral versus central MOR in the morphine-induced itch, we tested the opioid receptor antagonist naloxone methiodide, which is unable to cross the blood–brain barrier (Tejada *et al.*, 2017; Xu *et al.*, 2020). Intraperitoneal blockade of peripheral MOR with naloxone methiodide did not alter morphine-induced scratching (Fig. 2A, $P = 0.1873$). This result is consistent with a previous study in non-human primates, supporting the predominant role of spinal MOR in opioid-induced itch (Ko *et al.*, 2004). In contrast, intrathecal pretreatment with naloxone methiodide totally abolished morphine-induced itch, indicating the involvement of central spinal MOR (Fig. 2B, $P = 0.0004$). This finding was confirmed by the observation of very mild changes in intrathecal morphine-induced scratches (Fig. 2C, $P = 0.2005$) or biting and licking (Fig. 2D, $P = 0.8769$) in mice with conditional knockout of MOR on TRPV1$^+$ sensory neurons. To determine the involvement of C-fibre nociceptors in opioid-induced itch, we treated mice with three injections of RTX, which ablated TRPV1$^+$ sensory neurons or their axonal terminals and produced heat insensitivity (Liu *et al.*, 2010*a*; Berta *et al.*, 2014). The RTX treatment did not alter the pruritus induced by intrathecal morphine in wild-type mice (Fig. 2E, $P = 0.3969$). Furthermore, intradermal injection of morphine (100 nmol) evoked a very mild itch response (average of 14 scratches in 30 min), and this response was not affected in *Vgat-Cre*; *Oprm1*$^{fl/fl}$ mice (Fig. 2F, $P = 0.3281$). These data suggest that intrathecal morphine-induced itch is specifically mediated by MOR on inhibitory interneurons in the spinal cord.

Intrathecal morphine induces antinociception via MOR on sensory neurons and excitatory neurons

Spinal delivery of opioids is widely used in the clinical setting to provide analgesia. We likewise tested intrathecal morphine-induced antinociception in MOR conditional knockout mice. First, conditional knockout of MOR in TRPV1$^+$, Vgat$^+$, and SST$^+$ neurons does not change baseline tail-flick latency (Supplementary Fig. 1D, $P > 0.9999$, $P = 0.1324$, and $P = 0.2199$, respectively) or baseline hotplate paw withdrawal latency (Supplementary Fig. 1E, $P = 0.7716$, $P > 0.9999$, $P > 0.9999$, respectively). Conditional knockout of MOR in Vgat$^+$ neurons did not change baseline mechanical threshold (Supplementary Fig. 1F, $P = 0.4106$). In tail-flick testing, intrathecal morphine significantly increased tail-flick latency, and this antinociceptive effect was significantly reduced in *Sst-Cre*; *Oprm1*$^{fl/fl}$ mice (Fig. 3A, $P = 0.0016$), but not in *Vgat-Cre*; *Oprm1*$^{fl/fl}$ (Fig. 3A, $P = 0.4893$) or *Trpv1-Cre*; *Oprm1*$^{fl/fl}$ mice (Fig. 3A, $P = 0.0801$), although there was a weak decrease observed in *Trpv1-Cre*; *Oprm1*$^{fl/fl}$ mice. In hotplate testing, intrathecal morphine-induced antinociception was significantly decreased in both *Sst-Cre*; *Oprm1*$^{fl/fl}$ mice and *Trpv1-Cre*; *Oprm1*$^{fl/fl}$ mice (Fig. 3B, $P < 0.0001$ for both). Intrathecal morphine-induced antinociception was significantly enhanced and prolonged in *Vgat-cre*; *Oprm1*$^{fl/fl}$ mice (Fig. 3B, $P = 0.0050$). The dose response analysis revealed that of morphine antinociception was enhanced in *Vgat-Cre*; *Oprm1*$^{fl/fl}$ mice in the hotplate test but not in the tail-flack test (Fig. 3C and D). Taken together, these results indicate that intrathecal morphine-induced antinociception is mediated by MOR on spinal cord excitatory interneurons and peripheral sensory neurons.

MOR agonists suppress the activities of MOR$^+$ inhibitory interneurons in spinal cord slices

We next examined MOR expression in the SDH by RNAscope assay. *Oprm1* mRNA expression on excitatory and inhibitory neurons was tested by staining for *Oprm1* with Vglut2 (*Slc17a6*) mRNA in *Vgat*-Cre; Ai9 tdTomato mice. *Oprm1* expression was observed on both Vgat$^+$ and Vglut2$^+$ interneurons in lamina II of the SDH (Fig. 4A–C). This finding is in line with recent studies (Wang *et al.*, 2018; Zhang *et al.*, 2020) and published single cell sequencing data which demonstrated broad MOR expression in both inhibitory and excitatory interneurons of the SDH (Haring *et al.*, 2018).

Next, we performed *ex vivo* electrophysiology recordings of spinal cord slices to evaluate the effects of MOR agonists on inhibitory interneurons, as opioids activate potassium channels through G protein-coupled receptors to generate outward currents in MOR expressing neurons (North and Williams, 1985). DAMGO (0.5 μM) evoked outward

Figure 1 continued
licking was totally abolished in *Vgat-Cre*; *Oprm1*$^{fl/fl}$ mice. $P < 0.0001$ versus Cre-negative littermates, two-tailed Student's *t*-test. (**E**) Intrathecal morphine-induced scratches were not changed in *Sst-Cre*; *Oprm1*$^{fl/fl}$ mice. $P = 0.3653$, two-tailed Student's *t*-test. (**F**) Intrathecal morphine-induced biking and licking was not changed in *Sst-Cre*; *Oprm1*$^{fl/fl}$ mice. $P = 0.6824$, two-tailed Student's *t*-test. (**G**) Time course (*left*) and total scratch bouts (*right*) within 30 min after intrathecal injection of different doses of MOR selective agonist DAMGO in wild-type mice. (**H**) Intrathecal 0.03 nmol DAMGO induced itch was totally abolished in *Vgat-Cre*; *Oprm1*$^{fl/fl}$ mice. $P = 0.0075$ versus Cre-negative littermates, two-tailed Student's *t*-test. Data are mean ± SEM. Sample sizes are indicated in parentheses. WT = wild-type.

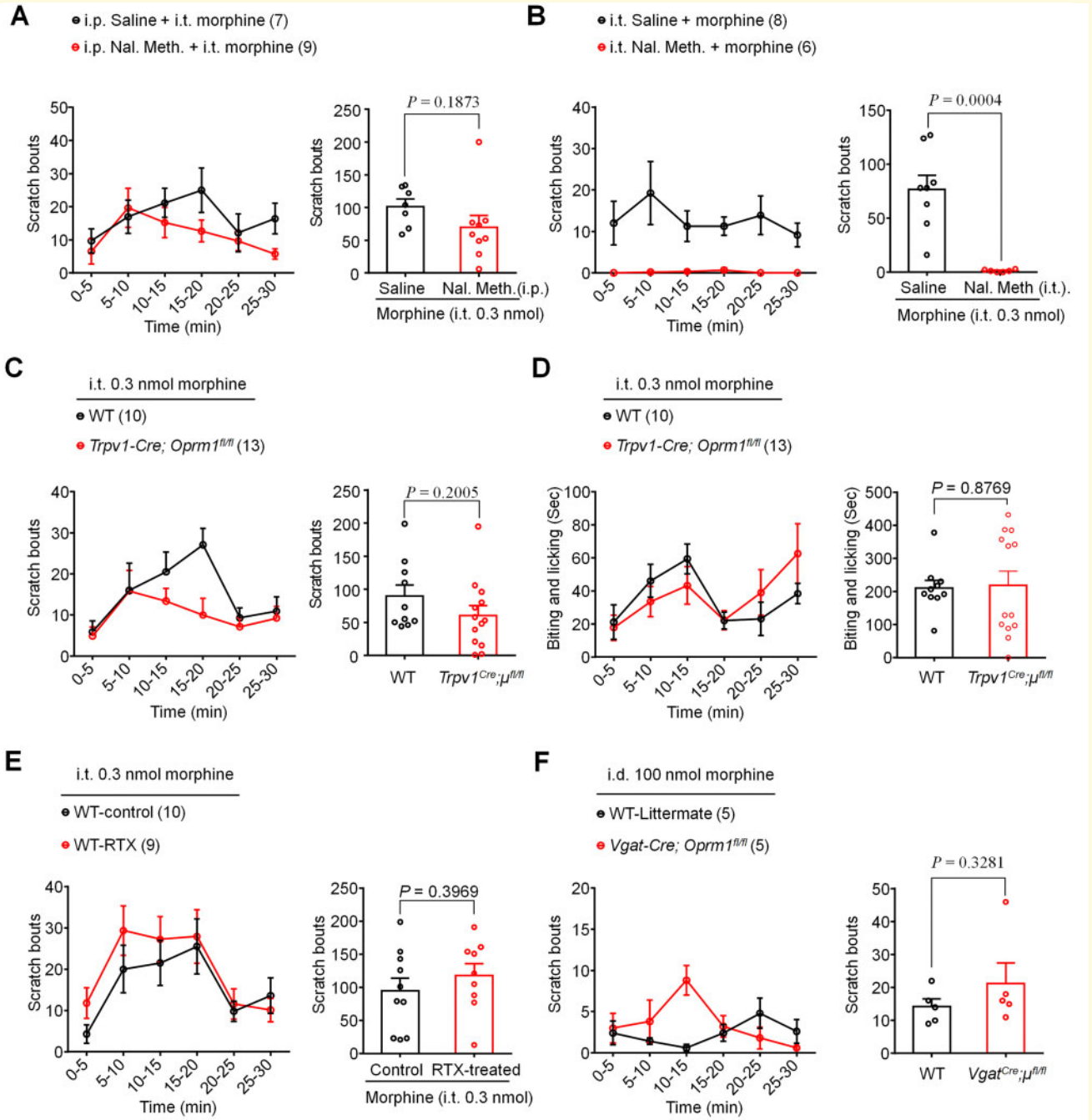

Figure 2 Intrathecal morphine-induced itch does not require peripheral MOR. (**A**) Intraperitoneal pretreatment with peripherally restricted MOR antagonist naloxone methiodide (10 mg/kg) did not affect itch induced by intrathecal (i.t.) morphine (0.3 nmol). $P = 0.1873$, two-tailed Student's *t*-test. (**B**) Pretreatment with naloxone methiodide (5 μg, i.t.) totally blocked intrathecal morphine-induced pruritus. $P = 0.0004$, two-tailed Student's *t*-test. (**C**) Intrathecal morphine-induced scratches were not altered in *Trpv1-Cre*; *Oprm1*$^{fl/fl}$ mice. $P = 0.2005$, two-tailed Student's *t*-test. (**D**) Intrathecal morphine-induced biting and licking was not altered in *Trpv1-Cre*; *Oprm1*$^{fl/fl}$ mice. $P = 0.8769$, two-tailed Student's *t*-test. (**E**) RTX treatment did not change intrathecal morphine-induced itch response. $P = 0.3969$, two-tailed Student's *t*-test. (**F**) Intradermal injection of morphine induced a very mild scratch response that was not affected in *Vgat-cre*; *Oprm1*$^{fl/fl}$ mice. $P = 0.3281$, two-tailed Student's *t*-test. Data are mean ± SEM. Sample sizes are indicated in parentheses.

currents in 9 of 19 SDH lamina II inhibitory interneurons with an amplitude of 15.9 pA in Vgat^{+} interneurons from *Vgat-Cre*; Ai9 tdTomato reporter mice (Fig. 5A). Morphine (10 μM) also significantly inhibited evoked action potentials in SDH lamina II inhibitory interneurons from the reporter mice (Fig. 5B and C, $P = 0.0109$).

To determine the role of morphine in inhibitory neurotransmission, we expressed channelrhodopsin ChR2 in

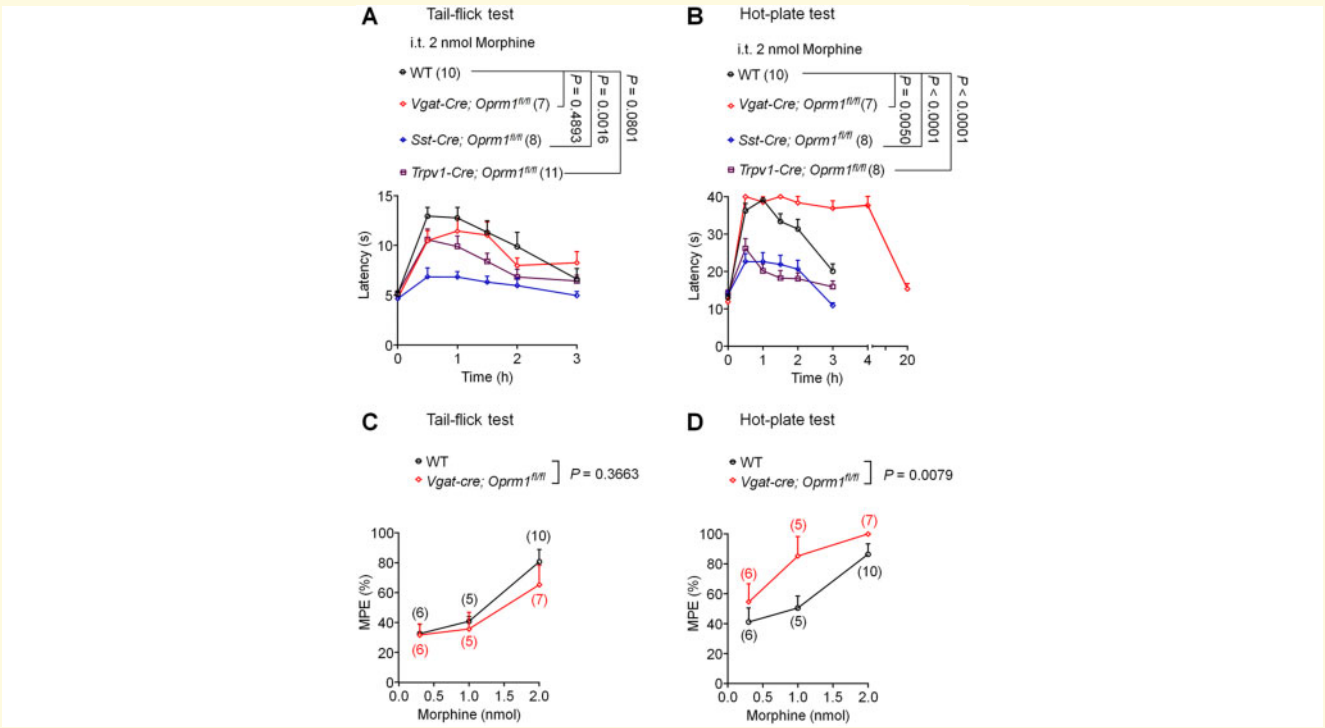

Figure 3 Intrathecal morphine-induced antinociception requires MOR expressed by spinal cord excitatory interneurons and peripheral sensory neurons. (**A**) Time course of morphine (2 nmol, i.t.) antinociception in tail-flick test in wild-type, *Vgat-Cre*; *Oprm1*$^{fl/fl}$, *Sst-Cre*; *Oprm1*$^{fl/fl}$, and *Trpv1-Cre*; *Oprm1*$^{fl/fl}$ mice. $P = 0.4893$, $P = 0.0016$, $P = 0.0801$, versus wild-type (WT) mice, two-way ANOVA. (**B**) Time course of morphine (2 nmol, i.t.) antinociception in the hotplate test in wild-type, *Vgat-Cre*; *Oprm1*$^{fl/fl}$, *Sst-Cre*; *Oprm1*$^{fl/fl}$, and *Trpv1-Cre*; *Oprm1*$^{fl/fl}$ mice. $P = 0.0050$, $P < 0.0001$, $P < 0.0001$, versus wild-type mice, two-way ANOVA. (**C**) Dose-response curve of morphine antinociception (MPE%) in the tail-flick test. $P = 0.3663$, versus wild-type mice, two-way ANOVA. (**D**) Dose-response curve of morphine antinociception (MPE%) in the hot-plate test. $P = 0.0079$, versus wild-type mice, two-way ANOVA. Data are mean ± SEM. Sample sizes are indicated in parentheses.

spinal Vgat$^+$ interneurons by crossing *Vgat*-Cre mice with Ai32 mice. We stimulated spinal Vgat$^+$ interneurons with 473 nm wavelength blue light and recorded the evoked IPSCs in lamina II Vgat$^-$ interneurons. Morphine (10 μM) significantly inhibited evoked IPSCs, indicating a functional inhibition of inhibitory interneurons (Fig. 5D and E, $P < 0.0001$). These results demonstrate that μ-opioids can directly inhibit the activities of MOR$^+$ inhibitory interneurons, suggesting that opioid-induced itch is a result of disinhibition.

Intrathecal morphine induced itch is suppressed by NPY and abolished by ablation of GRPR$^+$ interneurons

Two populations of SDH inhibitory interneurons, namely NPY$^+$ and dynorphin (DYN)$^+$ interneurons, have been implicated in the gate control of itch transmission (Ross *et al.*, 2010; Kardon *et al.*, 2014; Bourane *et al.*, 2015; Acton *et al.*, 2019; Pan *et al.*, 2019). We first examined *Oprm1* expression in these two populations of inhibitory interneurons by triple *in situ* hybridization for *Oprm1*, *Npy* and *Pdyn* mRNA expression in the SDH. We found that *Oprm1* in inhibitory interneurons is highly co-expressed in *Npy*$^+$ interneurons (Supplementary Fig. 2A and B). There is 38% of *Oprm1*$^+$ interneurons expressing *Npy*, 16% of positive interneurons expressing *Pdyn*, and 7% of *Oprm1*$^+$ interneurons expressing both *Npy* and dynorphin. Furthermore, we checked *Oprm1*, *Npy* mRNA expression in the SDH from *Vgat-Cre*; Ai9 tdTomato mice (Supplementary Fig. 3A and B). We found 45% of *Npy*$^+$ inhibitory interneurons expressing *Oprm1*, but only 13% of *Npy* negative inhibitory interneurons expressing. These data indicate *Oprm1* on inhibitory interneurons is mainly co-expressed with *Npy* (78%), and partially co-expressed with *Pdyn* (22%). This is consistent with data from a single-cell sequencing database (Supplementary Fig. 8) (Haring *et al.*, 2018). Notably, intrathecal co-administration of NPY (10 μg) with morphine (0.3 nmol) significantly inhibited morphine-induced itch (Fig. 6A, $P < 0.0001$). Spinal NPY-Y1 receptor is involved in itch transmission (Acton *et al.*, 2019). We observed that *Npy1r* is highly co-expressed with *Grp* (70%) (Supplementary Fig. 4). The expression patterns of

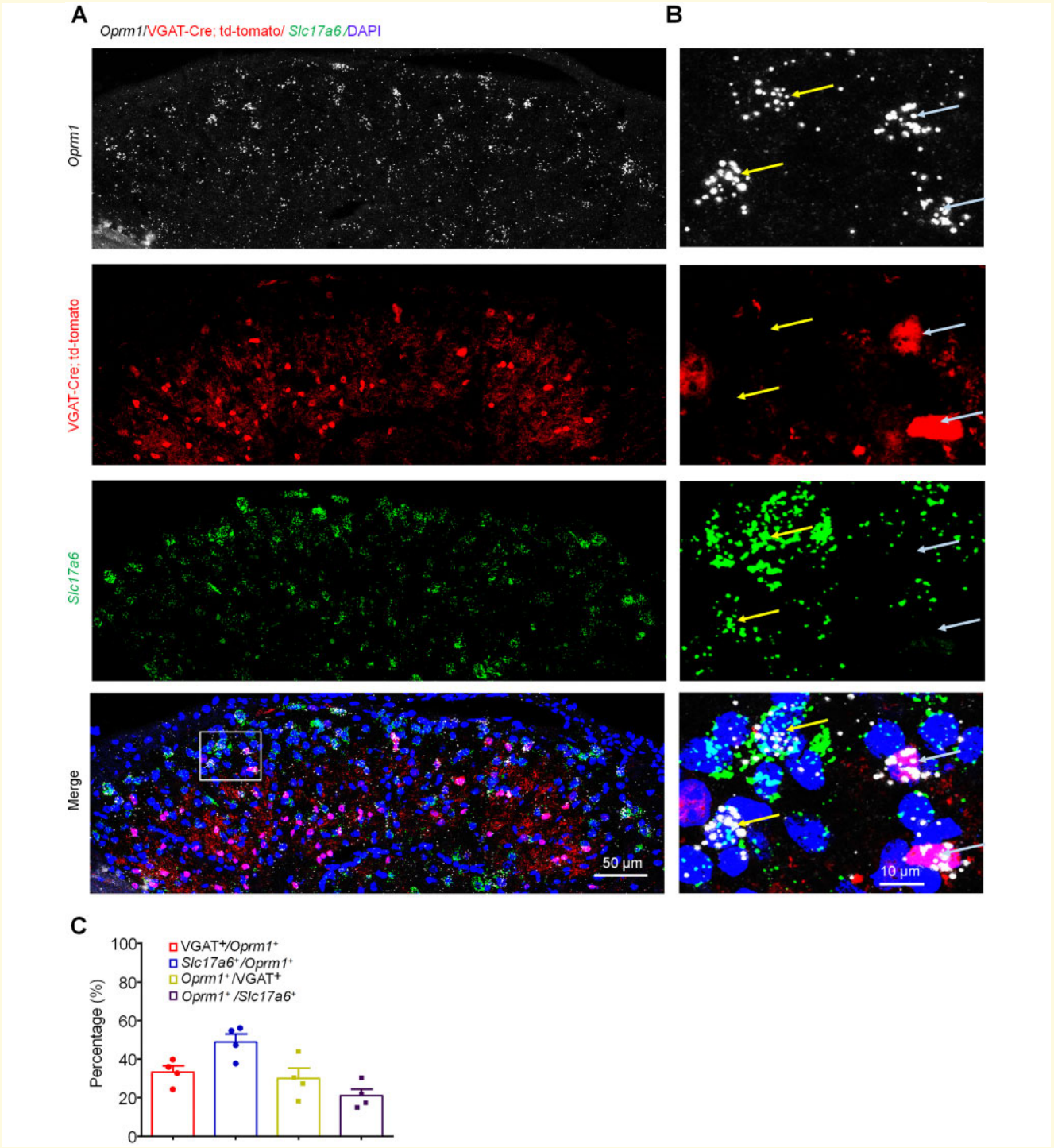

Figure 4 MOR is expressed by both inhibitory and excitatory interneurons in SDH. (**A** and **B**) *In situ* hybridization RNAscope images of MOR mRNA (*Oprm1*, white) and Vglut2 mRNA (*Slc17a6*, green) in mouse SDH of *Vgat-Cre*; *tdTomato* mice. Yellow arrows and white arrows indicate *Oprm1* double-labelled with Vglut2 or Vgat, respectively. Scale bar = 50 μm in **A**; 10 μm in **B**. (**C**) The percentage of co-expression between MOR and Vgat or Vglut2 neurons in SDH. Eight spinal cord sections from four mice were analysed. Data are mean ± SEM.

Oprm1, *Npy*, and *Npy1r* together suggest that MOR activation in NPY^+ inhibitory interneurons may disinhibit GRP^+ interneurons to produce itch. To test this hypothesis, we intrathecally injected bombesin-saporin (400 ng) to ablate $GRPR^+$ interneurons in SDH, as previously reported (Liu *et al.*, 2011; Pan *et al.*, 2019). Our RNAscope experiment confirmed that after the toxin treatment, the number of $Grpr^+$ neurons reduced by 97% at the lumbar level

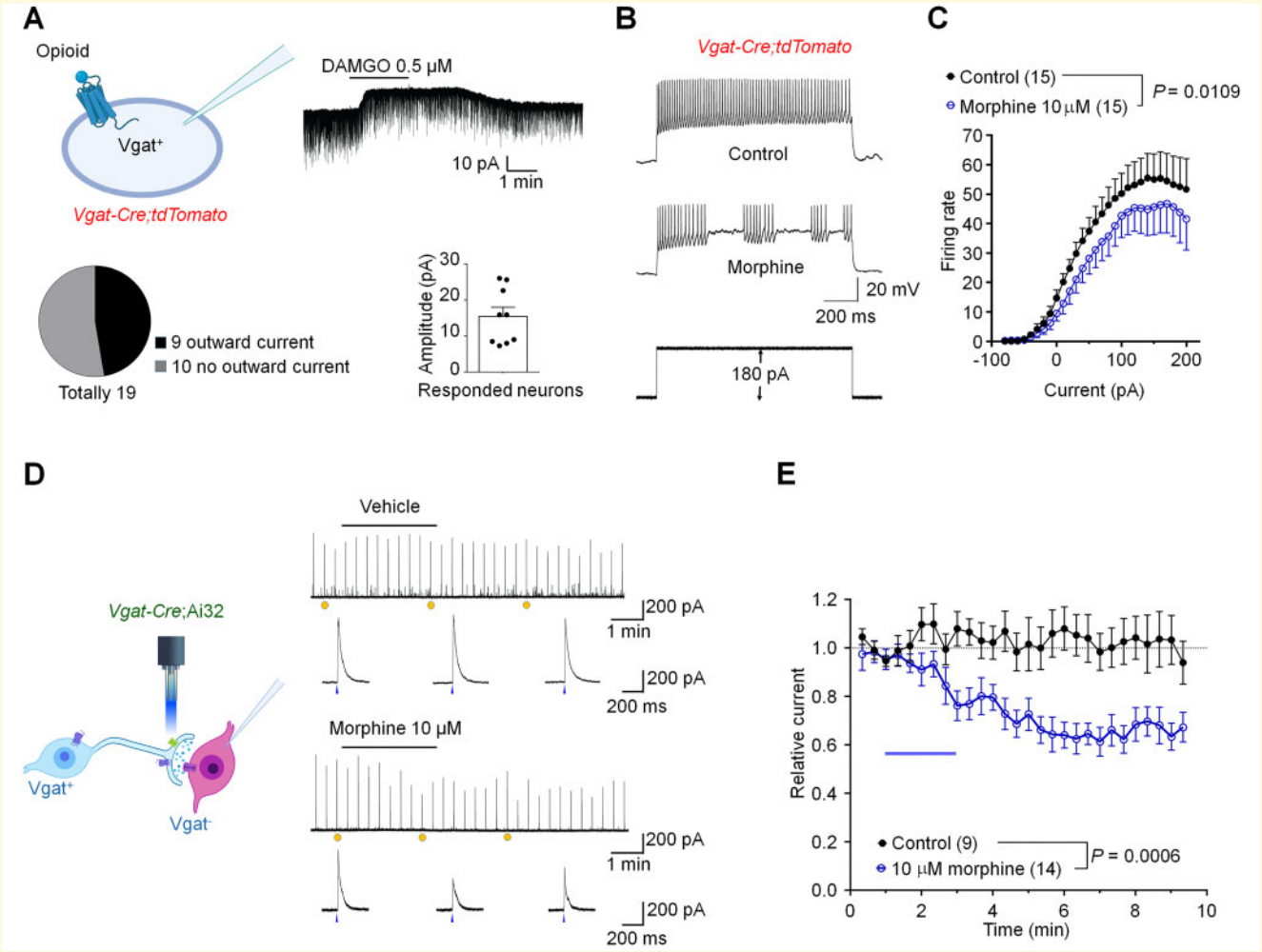

Figure 5 DAMGO and morphine inhibit the activities of MOR$^+$ inhibitory interneurons in SDH of spinal cord slices. (**A**) DAMGO (0.5 μM) induced outward currents recorded from Vgat$^+$ interneurons in the SDH from *Vgat-Cre*; *tdTomato* mice. Of 19 recorded neurons, nine showed outward currents with an average current of 15.9 pA. (**B**) Typical trace of action potentials from Vgat$^+$ interneurons in the spinal cord dorsal horn from *Vgat-Cre*; *tdTomato* mice. (**C**) Quantification of the effects of morphine (10 μM) on action potentials, $P = 0.0109$, two-way ANOVA. (**D**) Traces of light-evoked IPSCs in the spinal cord from *Vgat-Cre*; *Ai32* mice treated with vehicle (*top*) or morphine (*bottom*). (**E**) Quantification of morphine (10 μM) effects on evoked IPSC, $P = 0.0006$, two-way ANOVA. Data are mean ± SEM. Sample sizes are indicated in parentheses.

(Supplementary Fig. 5) and 91% at the cervical level (Supplementary Fig. 6). However, the number of *Oprm1*$^+$ neurons did not change after the ablation (Supplementary Figs 5 and 6). In bombesin-saporin pretreated mice, the pruritus evoked by intrathecal GRP (0.1 nmol) was abolished, indicating a functional blockade of GRPR$^+$ interneurons (Fig. 6B, $P = 0.0049$). Notably, intrathecal morphine-induced itch was totally abolished by the toxin, suggesting an essential role of GRPR$^+$ interneurons in morphine-induced itch (Fig. 6C, $P = 0.0072$). In contrast, intrathecal GRP-induced itch was not affected in *Vgat-Cre*; *Oprm1*$^{fl/fl}$ mice (Fig. 6D, $P = 0.7797$). RNAscope analysis revealed very limited co-expression of *Oprm1* with *Grpr* (4.7%) in SDH (Supplementary Fig. 7), in agreement with single-cell sequencing data (Supplementary Fig. 8) (Haring *et al.*, 2018). Taken together, these data indicate that the action of GRP/GRPR may lie downstream of MOR$^+$ inhibitory interneurons in the production of intrathecal morphine-induced itch.

MOR in inhibitory interneurons contributes to dermatitis-associated persistent itch

We further investigated the contribution of MOR to itch in different animal models of pruritus. We first used a DNFB-induced allergic contact dermatitis model (Liu *et al.*, 2016) to determine the roles of MOR in chronic itch. DNFB-induced itch was significantly reduced in *Vgat-Cre*; *Oprm1*$^{fl/fl}$ mice (Fig. 7A and B, $P = 0.0224$). Moreover, we tested acute itch induced by chloroquine and histamine.

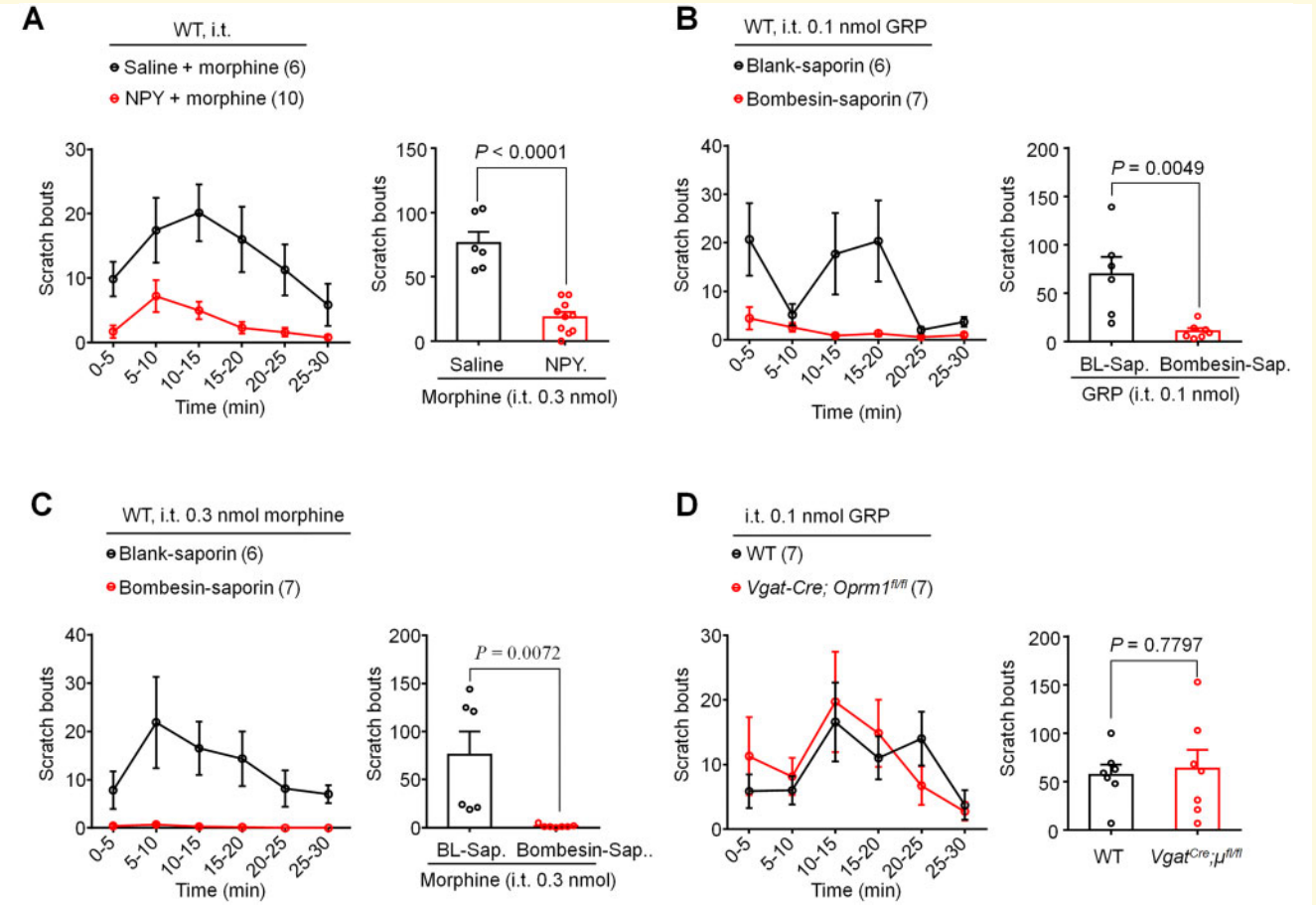

Figure 6 Morphine-induced itch is suppressed by intrathecal NPY and ablation of GRPR$^+$ neurons. (**A**) Intrathecal (i.t.) morphine (0.3 nmol) induced itch is inhibited by co-injection of NPY (10 μg, i.t.) in wild-type (WT) mice. $P < 0.0001$, two-tailed Student's *t*-test. (**B**) Intrathecal GRP (0.1 nmol) induced itch is abolished by ablation of spinal GRPR$^+$ neurons via intrathecal injection of bombesin-saporin (400 ng). $P = 0.0049$, two-tailed Student's *t*-test. (**C**) Intrathecal morphine (0.3 nmol) induced itch is abolished in bombesin-saporin treatment. $P = 0.0072$, two-tailed Student's *t*-test. (**D**) Intrathecal GRP (0.1 nmol) induced itch is not affected in *Vgat-Cre*; *Oprm1*$^{fl/fl}$ mice. $P = 0.7797$, two-tailed Student's *t*-test. Data are mean ± SEM.

Acute itch induced by intradermal injection of histamine and chloroquine did not significantly change in *Vgat-Cre*; *Oprm1*$^{fl/fl}$ mice (Fig. 7C and D, $P = 0.8002$, $P = 0.6328$, respectively). Furthermore, we tested weather subthreshold of morphine can enhance these pruritogens induced itch. The low-dose morphine (0.03 nmol) could enhance chemical itch provoked by histamine but not chloroquine (Fig. 7E and F, $P = 0.0391$ and $P = 0.7856$, respectively). These results indicate that MOR on inhibitory interneurons also regulates chronic itch in dermatitis.

A centrally-restricted MOR antagonist inhibits dermatitis and lymphoma-induced chronic itch

We used the peripherally-restricted opioid receptor antagonist naloxone methiodide to assess the role of peripherally expressed MOR in dermatitis-induced persistent itch. Intraperitoneal injection of naloxone but not naloxone methiodide significantly reduced spontaneous itch in the DNFB model suggesting that MOR expressed in the CNS more critically involved in chronic itch (Fig 8A, $P = 0.0044$ and $P = 0.6383$, respectively). Furthermore, intrathecal naloxone significantly reduced DNFB-induced itch (Fig. 8B, $P = 0.0007$).

Finally, we tested opioid antagonists in a mouse CTCL model, which was recently developed in our lab by intradermal inoculation of human MyLa cells (Han *et al.*, 2018). In the CTCL model, mice develop lymphoma and chronic itch (Han *et al.*, 2018). Similar to the results found in the DNFB model, only systemic treatment with naloxone but not peripherally restricted naloxone methiodide significantly inhibited spontaneous itch in CTCL mice (Fig. 8C, $P < 0.0001$ and $P = 0.2987$, respectively). Intrathecally injected naloxone also significantly abolished spontaneous itch in the CTCL model (Fig. 8D, $P = 0.0001$). These results indicate that centrally but not peripherally expressed MOR plays a major role in dermatitis and lymphoma-induced chronic itch.

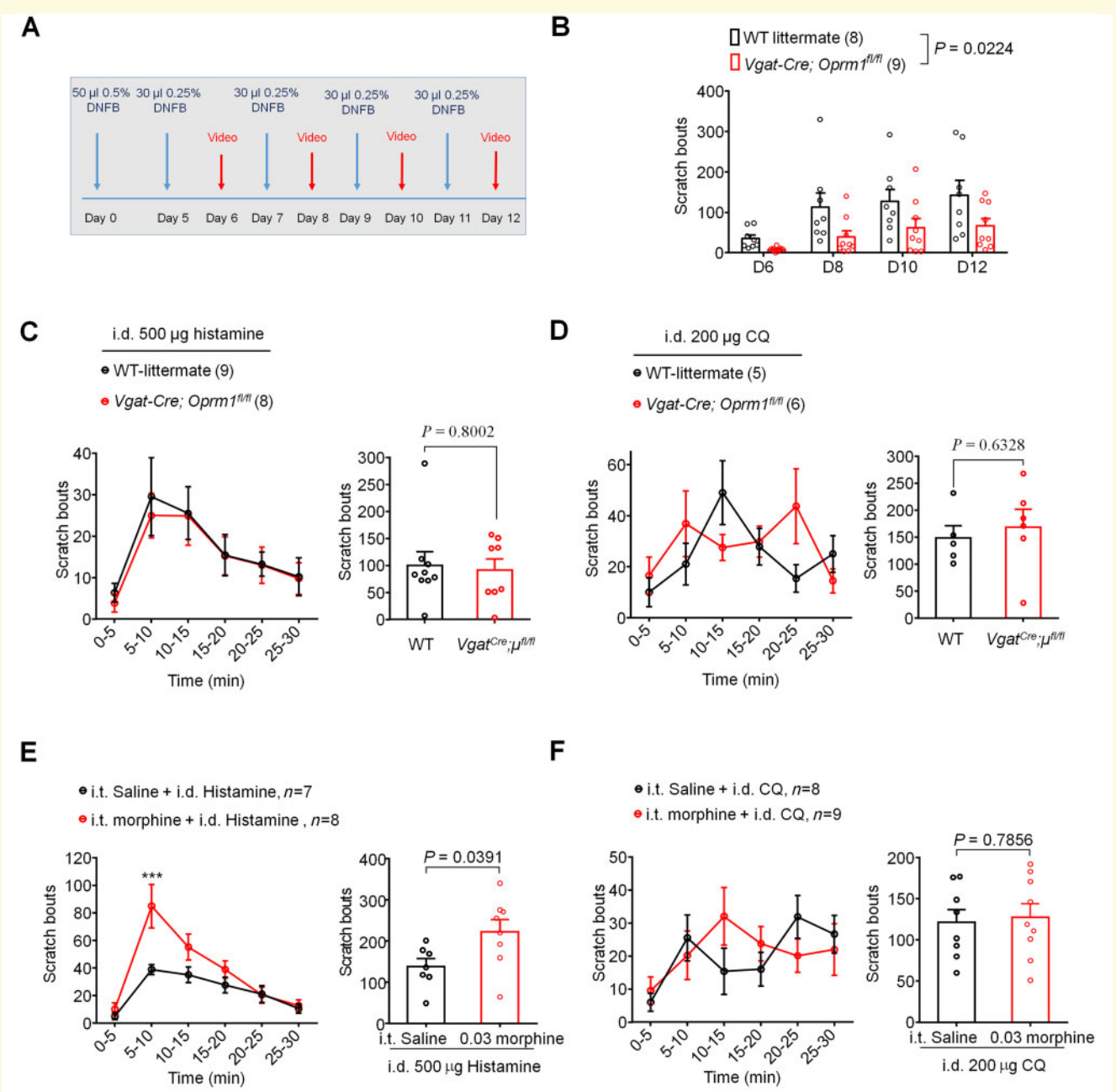

Figure 7 MOR on inhibitory neurons regulates chronic itch. (**A**) Protocol of experimental design for the DNFB mouse model. (**B**) Spontaneous itch in the DNFB mouse model is significantly decreased in *Vgat-Cre*; *Oprm1*$^{fl/fl}$ mice. $P = 0.0224$, two-way ANOVA. (**C**) Time course of scratch bouts (*left*) and total scratch bouts (*right*) within 30 min after intradermal injection of 500 µg histamine in wild-type (WT) and *Vgat-Cre*; *Oprm1*$^{fl/fl}$ mice. $P = 0.8002$, two-tailed Student's *t*-test. (**D**) Time course of scratch bouts (*left*) and total scratch bouts (*right*) within 30 min after intradermal injection of 200 µg chloroquine in wild-type and *Vgat-Cre*; *Oprm1*$^{fl/fl}$ mice. $P = 0.6328$, two-tailed Student's *t*-test. (**E**) Time course of scratch bouts (*left*) and total scratch bouts (*right*) within 30 min after intrathecal injection of saline or 0.03 nmol morphine followed by intradermal injection of 500 µg histamine in wild-type mice. $P = 0.0391$, two-tailed Student's *t*-test. (**F**) Time course of scratch bouts (*left*) and total scratch bouts (*right*) within 30 min after intrathecal injection of saline or 0.03 nmol morphine followed by intradermal injection of 200 µg chloroquine in wild-type mice. $P = 0.7856$, two-tailed Student's *t*-test. Data are mean ± SEM. Sample sizes are indicated in parentheses.

Discussion

Itch is a common side effect of opioids. In this study, we demonstrated that intrathecal µ-opioids such as morphine and DAMGO elicited itch responses that are mediated by MOR on spinal GABAergic inhibitory interneurons. µ-opioids inhibited the activities of Vgat$^+$ interneurons in the spinal cord and disinhibited the itch signalling pathway, resulting in pruritus. Additionally, chronic itch in the DNFB-induced allergic contact dermatitis mouse model was

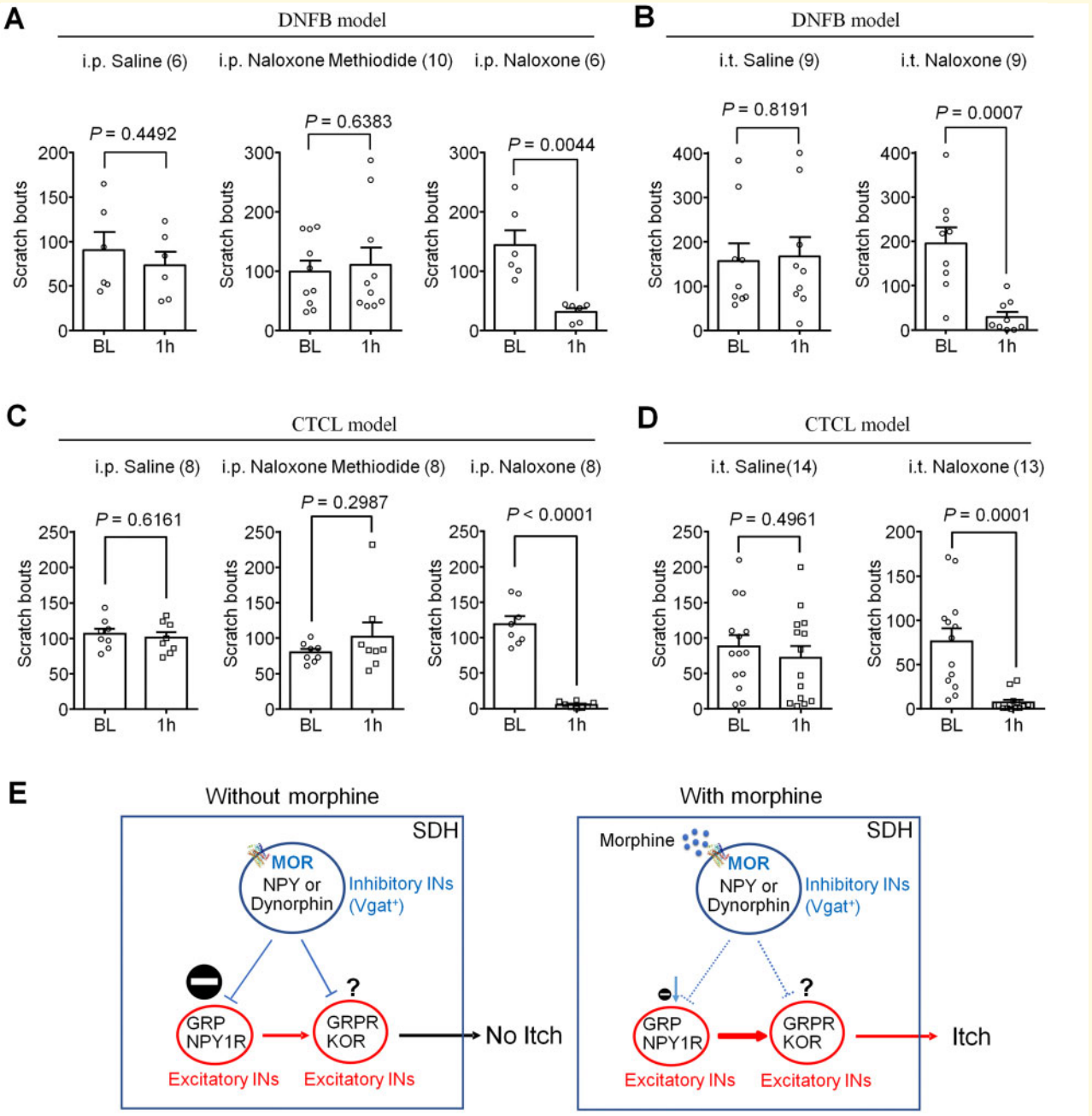

Figure 8 Central MOR contributes to chronic itch in the DNFB model and CTCL model. (**A**) Effects of intraperitoneal (i.p.) pretreatment with saline, naloxone methiodide, or naloxone on DNFB-induced itch. $P = 0.4492$, $P = 0.6383$, and $P = 0.0044$, respectively, two-tailed Student's *t*-test. (**B**) The effects of intrathecal (i.t.) pretreatment with saline or naloxone on DNFB-induced spontaneous itch. $P = 0.8191$ and $P = 0.0007$, respectively, two-tailed Student's *t*-test. (**C**) The effects of intraperitoneal pretreatment with saline, naloxone methiodide, or naloxone, on spontaneous itch in the CTCL model. $P = 0.6161$, $P = 0.2987$, and $P < 0.0001$, respectively, two-tailed Student's *t*-test. (**D**) The effects of intrathecal pretreatment with saline, or naloxone on CTCL-induced chronic itch. $P = 0.4961$ and $P = 0.0001$, respectively, two-tailed Student's *t*-test. Data are mean ± SEM. Sample sizes are indicated in parentheses. (**E**) Schematic of working hypothesis. *Left*: In the absence of morphine, NPY^+ or dynorphin$^+$ inhibitory interneurons suppress itch circuit by inhibiting GRP^+ and $GRPR^+$ excitatory interneurons. *Right*: Morphine acts on MORs expressed on NPY^+ or dynorphin$^+$ inhibitory interneurons and causes disinhibition of GRP^+ and $GRPR^+$ excitatory interneurons to elicit itch. MOR is also expressed on excitatory neurons and other inhibitory neurons in SDH. BL = baseline; INs = interneurons.

decreased after *Oprm1-Vgat* deletion. Finally, naloxone, but not peripherally-restricted naloxone methiodide, inhibited itch in the DNFB dermatitis model and the CTCL cancer itch model, indicating the contribution of central MORs to chronic itch. Our findings demonstrate that intrathecal opioid acts upon MORs on spinal inhibitory interneurons to

evoke pruritus via disinhibition. Our data also suggest that chronic itch could be effectively treated with CNS-targeted naloxone.

Recent progress has advanced our understanding regarding the mechanisms of itch (LaMotte *et al.*, 2014; Ji, 2018; Cevikbas and Lerner, 2019). The itch sensation is initiated by the activation of distinct populations of primary pruriceptors expressing MAS-related GPR receptors (Mrgpr), histamine receptors, 5-HT receptors, and natriuretic peptide B (NPPB) by a variety of pruritogens (Liu *et al.*, 2009; Han *et al.*, 2013; Mishra and Hoon, 2013; Pan *et al.*, 2019). The pruriceptors transmit itch signals to the spinal cord by release of neuropeptides such as NPPB in the SDH (Mishra and Hoon, 2013, but also see Sun and Chen, 2007). The spinal interneurons expressing natriuretic peptide receptor 1 (NPR1) and GRP receive and process chemical itch signals (Sun and Chen, 2007; Sun *et al.*, 2009; Mishra and Hoon, 2013; LaMotte *et al.*, 2014). Like mechanical allodynia, mechanical itch could be mediated by a subtype of Aβ low-threshold mechanoreceptors expressing Toll-like receptor 5 (TLR5), transmitting itch signals to a subpopulation of excitatory interneurons expressing urocortin 3 or NPY1R (Pan *et al.*, 2019; Wang *et al.*, 2019). Furthermore, two populations of inhibitory interneurons expressing Bhlhb5$^+$ and NPY$^+$ in the SDH are involved in modulating chemical and mechanical itch, respectively (Ross *et al.*, 2010; Bourane *et al.*, 2015; Acton *et al.*, 2019; Pan *et al.*, 2019). While recent studies support 'labelled line' theory by identifying several populations of pruriceptive sensory neurons and GRPR$^+$ spinal cord neurons, they also support 'population coding' theory (Ma, 2012; LaMotte *et al.*, 2014). According to 'population coding', labelled lines are interconnected through local excitatory and inhibitory interneurons. As a result, activation of one labelled line could modulate, or provide gate control of, another labelled line (Ma, 2012). In particular, pain is known to suppress itch via spinal thalamic tract neurons. In monkeys, the responses of pruriceptive spinal thalamic tract neurons to histamine are suppressed when the skin is scratched. Interestingly, in the same neurons capsaicin-induced responses are increased by scratching (Davidson *et al.*, 2009). In mice, responses of dorsal horn neurons to pruritogens are decreased by scratching and this effect is mediated GABAergic transmission (Akiyama *et al.*, 2011). Deletion of the vGluT2 population of nociceptive neurons resulted in spontaneous itch and a loss of the inhibition of itch by pain such that an intradermal injection of capsaicin (normally painful) evoked itch and not pain behaviour (Liu *et al.*, 2010*b*). Noxious or cooling agents inhibit the activity of spinal GRPR$^+$ neurons via GABAergic signalling (Bardoni *et al.*, 2019).

Despite the progress in revealing neurocircuits of itch, the specific roles of MOR in itch signalling remained unclear. In support of 'population coding' and 'pain suppression of itch', intrathecal morphine induces paradoxical itch and analgesia, and different populations of projection neurons (e.g. trigeminothalamic tract neurons) are involved in intrathecal morphine-induced itch and analgesia. Notably, morphine caused excitation and increased the responses of pruriceptive neurons to a chemical pruritogen, meanwhile suppressing the non-pruriceptive neurons that selectively transmitted signals elicited by painful stimuli (Moser and Giesler, 2013). It is also worthwhile to mention that Liu *et al.* (2011) demonstrated that morphine-induced analgesia and itch are mediated in parallel by different MOR isoforms, MOR1 for analgesia and MOR1D for itch. Mechanistically, MOR1D forms heterodimer with GRPR, and activation of MOR1D by morphine results in further activation of the GRPR-expressing pruriceptive neurons (Liu *et al.*, 2011). In contrast, our findings suggest that intrathecal morphine elicits itch via disinhibition (Fig. 8E). Strikingly, we found that conditional deletion of *Oprm1* in Vgat$^+$ inhibitory neurons completely abolished pruritus induced by intrathecal morphine or DAMGO (Fig. 1C and H). In support of Liu's study (Liu *et al.*, 2011), our result also shows that GRPR$^+$ neurons are critically essential for morphine-induced pruritus (Fig. 6C).

Our data also showed that intrathecal morphine-evoked itch and antinociception is mediated by different populations of interneurons, specifically excitatory interneurons for antinociception and inhibitory neurons for pruritus. Deletion of MOR in SST$^+$ excitatory interneurons had no effect on morphine induced itch. In the SDH, majority of SST$^+$ interneurons are excitatory (Chamessian *et al.*, 2018; Duan *et al.*, 2018; Huang *et al.*, 2018), but we cannot exclude the possibility that some SST$^+$ neurons are inhibitory. Notably, loss of MOR in SST$^+$ interneurons resulted in a substantial reduction (80%) in morphine-induced antinociception. Mechanistically, morphine binds to MOR on excitatory interneurons to suppress neuronal activity by inducing outward currents through inwardly rectifying potassium channels (North and Williams, 1985; Andrade *et al.*, 2010). A previous report indicated primary afferent neurons in mice lacked GIRK channels (Nockemann *et al.*, 2013). Instead, morphine inhibits calcium channels on primary afferent neurons, and therefore, inhibits neurotransmitter release in SDH neurons via presynaptic regulation (Wang *et al.*, 2020). Of interest, loss of MOR in TRPV1$^+$ neurons did not affect morphine induced itch. This loss also resulted in a partial reduction of intrathecal morphine antinociception. Our data indicated that loss of MOR in inhibitory neurons (Vgat$^+$) enhanced and prolonged morphine antinociception in the hotplate test. Notably, a recent study suggested MOR on excitatory and inhibitory neurons has opposite roles in morphine antinociception: intrathecal morphine induced antinociception was mediated by MOR on excitatory neurons, whereas activation of MORs on spinal GABAergic neurons induced hyperalgesia (Zhang *et al.*, 2020).

Recent studies indicate GRPR$^+$ neurons are excitatory interneurons connected to NK1$^+$ projection neurons (Wang *et al.*, 2013; Mu *et al.*, 2017; Acton *et al.*, 2019; Bardoni *et al.*, 2019). Consistently, itch is abolished by ablation of NK1$^+$ projection neurons (Carstens *et al.*, 2010). Although our results indicated that ablation of GRPR$^+$ neurons totally blocked morphine-induced itch, as previously reported

(Liu *et al.*, 2011), this ablation did not affect the number of *Oprm1*-expressing neurons in SDH. Consistently, our *in situ* data showed limited co-localization of *Oprm1* and *Grpr* (<5%). Single-cell analysis in SDH neurons also revealed expression of *Oprm1* in inhibitory neurons and very limited co-expression of *Oprm1* and *Grpr* (Haring *et al.*, 2018) (Supplementary Fig. 8). Additionally, GRP-induced pruritus was not altered after *Oprm1* deletion in inhibitory neurons. Thus, GRPR$^+$ neurons might be downstream of the pathway for morphine-induced itch. Furthermore, our electrophysiological data confirmed that MOR agonists directly act on Vgat$^+$ inhibitory neurons to induce outward currents and suppress action potentials on inhibitory neurons (Fig. 5A–C), and importantly, morphine produce sustained inhibition of IPSCs on postsynaptic Vgat$^-$ excitatory neurons leading to disinhibition (Fig. 5D and E).

NPY was reported to modulate mechanical itch and histamine-induce itch (Gao *et al.*, 2018; Acton *et al.*, 2019; Pan *et al.*, 2019), but it remained unclear if NPY contributes to morphine-induced itch. Our *in situ* hybridization and behavioural data demonstrated that (i) *Oprm1* is co-expressed with both Vgat and NPY; (ii) intrathecal NPY effectively inhibited morphine-induced itch; and (iii) NPY1R is highly co-expressed with GRP in SDH neurons. Thus, we postulate that morphine activates MOR in NPY$^+$ inhibitory interneurons to disinhibit GRP$^+$ excitatory interneurons for pruritus (Fig. 8E).

There are also limitations of this study. First, morphine may act on GRP$^+$ excitatory interneurons to suppress the activities of a subset of GRP$^+$ neurons. Our RNAscope data indicate *Oprm1* expression in 30% GRP$^+$ neurons. However, a recent study indicated that most GRP$^+$ neurons showed response to DAMGO by exhibiting outward currents in GRP-EGFP mice (Dickie *et al.*, 2019), raising a possibility that the population of the functional MOR in GRP$^+$ neurons could be larger. A recent study proposed a 'leaky gate' hypothesis: *Grp*$^+$ neurons positively code for itch while negatively regulating pain transmission (Sun *et al.*, 2017). Future studies are warranted to determine how morphine regulates itch and pain through *Grp*$^+$ neurons. It will be of great interest to test whether direct inhibition of a subset of GRP$^+$ neurons is also essential for morphine to induce itch, as a lateral inhibition in sensory coding. Second, previous studies showed that kappa opioid receptor also contributes to morphine-induced itch in primates (Umeuchi *et al.*, 2003; Ko and Husbands, 2009; Lee and Ko, 2015). Nalfurafine, a KOR agonist, was reported to suppress morphine induced itch (Ruan *et al.*, 2016; Sakakihara *et al.*, 2016). Our *in situ* hybridization data revealed a moderate co-expression (16%) of *Pdyn* with *Oprm1* in mouse SDH (Supplementary Fig. 2). Thus, Both *Npy*$^+$ and *Pdyn*$^+$ inhibitory neurons may participant in morphine induced itch (Fig. 8E). Further identification of opioid receptor-containing inhibitory interneuron subtypes in opioid-induced itch remains an important area for future research.

Patients with chronic itch commonly experience high sensitivity to pruritogens, mechanically evoked itch sensations, and spontaneous itch (Ikoma *et al.*, 2006; LaMotte *et al.*, 2014). Opioid receptor antagonists including naloxone, naltrexone, and nalbuphine have been demonstrated to be the effective in treating chronic itch under certain pathological conditions (Brune *et al.*, 2004; Reszke and Szepietowski, 2018; Serrano *et al.*, 2018; Kremer, 2019). MOR antagonists are effective in alleviating dermatitis-associated itch (Monroe, 1989; Metze *et al.*, 1999; Farmer and Marathe, 2017; Pavlis and Yosipovitch, 2018; Ekelem *et al.*, 2019). Naltrexone relieves uremic pruritus in patients with chronic kidney disease (Peer *et al.*, 1996; Legroux-Crespel *et al.*, 2004). Furthermore, case reports have shown that naloxone and naltrexone are effective therapies for anti-PD1 immunotherapy-induced pruritus (Kwatra *et al.*, 2018; Singh *et al.*, 2019). Our study revealed that pruritus in DNFB-induced allergic contact dermatitis is significantly impaired under the conditional deletion of MOR in GABAergic neurons. Furthermore, naloxone but not peripherally-restricted naloxone methiodide effectively alleviated chronic itch in DNFB-induced allergic contact dermatitis and lymphoma-induced cancer itch models. Further clinical studies will be needed to test the effects of intrathecal or CNS-penetrating MOR antagonists in patients suffering from various chronic itch conditions.

Funding

This study was supported by Duke University funds.

Competing interests

R-R.J. is a consultant of Boston Scientific and received research support from the company. These activities are not related to this study.

Supplementary material

Supplementary material is available at *Brain* online.

References

Acton D, Ren X, Di Costanzo S, Dalet A, Bourane S, Bertocchi I, et al. Spinal neuropeptide Y1 receptor-expressing neurons form an essential excitatory pathway for mechanical itch. Cell Rep 2019; 28: 625–39 e6.

Akiyama T, Iodi Carstens M, Carstens E. Transmitters and pathways mediating inhibition of spinal itch-signaling neurons by scratching and other counterstimuli. PLoS One 2011; 6: e22665.

Andrade A, Denome S, Jiang Y-Q, Marangoudakis S, Lipscombe D.Opioid inhibition of N-type Ca^{2+} channels and spinal analgesia couple to alternative splicing. Nat Neurosci 2010; 13: 1249–56. 10.1038/nn.2643

Bardoni R, Shen KF, Li H, Jeffry J, Barry DM, Comitato A, et al. Pain inhibits GRPR neurons via GABAergic signaling in the spinal cord. Sci Rep 2019; 9: 15804.

Berta T, Park CK, Xu ZZ, Xie RG, Liu T, Lu N, et al. Extracellular caspase-6 drives murine inflammatory pain via microglial TNF-alpha secretion. J Clin Invest 2014; 124: 1173–86.
Bourane S, Duan B, Koch SC, Dalet A, Britz O, Garcia-Campmany L, et al. Gate control of mechanical itch by a subpopulation of spinal cord interneurons. Science 2015; 350: 550–4.
Brune A, Metze D, Luger TA, Ständer S. Antipruritic therapy with the oral opioid receptor antagonist naltrexone. Open, non-placebo controlled administration in 133 patients. Hautarzt 2004; 55: 1130–6.
Carstens EE, Carstens MI, Simons CT, Jinks SL. Dorsal horn neurons expressing NK-1 receptors mediate scratching in rats. Neuroreport 2010; 21: 303–8.
Cevikbas F, Lerner EA. Physiology and pathophysiology of itch. Physiol Rev 2019; 100: 945–82.
Chamessian A, Young M, Qadri Y, Berta T, Ji RR, Van de Ven T. Transcriptional profiling of somatostatin interneurons in the spinal dorsal horn. Sci Rep 2018; 8: 6809.
Chen G, Kim YH, Li H, Luo H, Liu D-L, Zhang Z-J, et al. PD-L1 inhibits acute and chronic pain by suppressing nociceptive neuron activity via PD-1. Nat Neurosci 2017; 20: 917–26.
Chen G, Park CK, Xie RG, Berta T, Nedergaard M, Ji RR. Connexin-43 induces chemokine release from spinal cord astrocytes to maintain late-phase neuropathic pain in mice. Brain 2014; 137: 2193–209.
Corder G, Castro DC, Bruchas MR, Scherrer G. Endogenous and exogenous opioids in pain. Annu Rev Neurosci 2018; 41: 453–73.
Davidson S, Zhang X, Khasabov SG, Simone DA, Giesler GJ Jr. Relief of itch by scratching: state-dependent inhibition of primate spinothalamic tract neurons. Nat Neurosci 2009; 12: 544–6.
Dickie AC, Bell AM, Iwagaki N, Polgar E, Gutierrez-Mecinas M, Kelly R, et al. Morphological and functional properties distinguish the substance P and gastrin-releasing peptide subsets of excitatory interneuron in the spinal cord dorsal horn. Pain 2019; 160: 442–62.
Duan B, Cheng L, Ma Q. Spinal circuits transmitting mechanical pain and itch. Neurosci Bull 2018; 34: 186–93.
Ekelem C, Juhasz M, Khera P, Mesinkovska NA. Utility of naltrexone treatment for chronic inflammatory dermatologic conditions: a systematic review. JAMA Dermatol 2019; 155: 229–36.
Farmer WS, Marathe KS. Atopic dermatitis: managing the itch. Adv Exp Med Biol 2017; 1027: 161–77.
Gao T, Ma H, Xu B, Bergman J, Larhammar D, Lagerstrom MC. The neuropeptide Y system regulates both mechanical and histaminergic itch. J Invest Dermatol 2018; 138: 2405–11.
Han L, Ma C, Liu Q, Weng HJ, Cui Y, Tang Z, et al. A subpopulation of nociceptors specifically linked to itch. Nat Neurosci 2013; 16: 174–82.
Han Q, Liu D, Convertino M, Wang Z, Jiang C, Kim YH, et al. miRNA-711 binds and activates TRPA1 extracellularly to evoke acute and chronic pruritus. Neuron 2018; 99: 449–63.e6.
Haring M, Zeisel A, Hochgerner H, Rinwa P, Jakobsson JET, Lonnerberg P, et al. Neuronal atlas of the dorsal horn defines its architecture and links sensory input to transcriptional cell types. Nat Neurosci 2018; 21: 869–80.
Huang J, Polgar E, Solinski HJ, Mishra SK, Tseng PY, Iwagaki N, et al. Circuit dissection of the role of somatostatin in itch and pain. Nat Neurosci 2018; 21: 707–16.
Hylden JL, Wilcox GL. Intrathecal morphine in mice: a new technique. Eur J Pharmacol 1980; 67: 313–6.
Ikoma A, Steinhoff M, Stander S, Yosipovitch G, Schmelz M. The neurobiology of itch. Nat Rev Neurosci 2006; 7: 535–47.
Ji RR. Recent progress in understanding the mechanisms of pain and itch: the second special issue. Neurosci Bull 2018; 34: 1–3.
Ji RR, Zhang Q, Law PY, Low HH, Elde R, Hokfelt T. Expression of mu-, delta-, and kappa-opioid receptor-like immunoreactivities in rat dorsal root ganglia after carrageenan-induced inflammation. J Neurosci 1995; 15: 8156–66.
Jiang CY, Fujita T, Kumamoto E. Synaptic modulation and inward current produced by oxytocin in substantia gelatinosa neurons of adult rat spinal cord slices. J Neurophysiol 2014; 111: 991–1007.
Kardon AP, Polgar E, Hachisuka J, Snyder LM, Cameron D, Savage S, et al. Dynorphin acts as a neuromodulator to inhibit itch in the dorsal horn of the spinal cord. Neuron 2014; 82: 573–86.
Ko MC, Husbands SM. Effects of atypical kappa-opioid receptor agonists on intrathecal morphine-induced itch and analgesia in primates. J Pharmacol Exp Ther 2009; 328: 193–200.
Ko MC, Song MS, Edwards T, Lee H, Naughton NN. The role of central mu opioid receptors in opioid-induced itch in primates. J Pharmacol Exp Ther 2004; 310: 169–76.
Kremer AE. What are new treatment concepts in systemic itch? Exp Dermatol 2019; 28: 1485–92.
Kumar K, Singh SI. Neuraxial opioid-induced pruritus: an update. J Anaesthesiol Clin Pharmacol 2013; 29: 303–7.
Kwatra SG, Stander S, Kang H. PD-1 blockade-induced pruritus treated with a mu-opioid receptor antagonist. N Engl J Med 2018; 379: 1578–9.
LaMotte RH, Dong X, Ringkamp M. Sensory neurons and circuits mediating itch. Nat Rev Neurosci 2014; 15: 19–31.
LaMotte RH, Shimada SG, Sikand P. Mouse models of acute, chemical itch and pain in humans. Exp Dermatol 2011; 20: 778–82.
Lee H, Ko MC. Distinct functions of opioid-related peptides and gastrin-releasing peptide in regulating itch and pain in the spinal cord of primates. Sci Rep 2015; 5: 11676.
Legroux-Crespel E, Cledes J, Misery L. A comparative study on the effects of naltrexone and loratadine on uremic pruritus. Dermatology 2004; 208: 326–30.
Liu Q, Tang Z, Surdenikova L, Kim S, Patel KN, Kim A, et al. Sensory neuron-specific GPCR Mrgprs are itch receptors mediating chloroquine-induced pruritus. Cell 2009; 139: 1353–65.
Liu T, Han Q, Chen G, Huang Y, Zhao LX, Berta T, et al. Toll-like receptor 4 contributes to chronic itch, alloknesis, and spinal astrocyte activation in male mice. Pain 2016; 157: 806–17.
Liu T, Xu ZZ, Park CK, Berta T, Ji RR. Toll-like receptor 7 mediates pruritus. Nat Neurosci 2010a; 13: 1460–2.
Liu XY, Liu ZC, Sun YG, Ross M, Kim S, Tsai FF, et al. Unidirectional cross-activation of GRPR by MOR1D uncouples itch and analgesia induced by opioids. Cell 2011; 147: 447–58.
Liu Y, Abdel Samad O, Zhang L, Duan B, Tong Q, Lopes C, et al. VGLUT2-dependent glutamate release from nociceptors is required to sense pain and suppress itch. Neuron 2010b; 68: 543–56.
Ma Q. Population coding of somatic sensations. Neurosci Bull 2012; 28: 91–9.
Matthes HW, Maldonado R, Simonin F, Valverde O, Slowe S, Kitchen I, et al. Loss of morphine-induced analgesia, reward effect and withdrawal symptoms in mice lacking the mu-opioid-receptor gene. Nature 1996; 383: 819–23.
Metze D, Reimann S, Beissert S, Luger T. Efficacy and safety of naltrexone, an oral opiate receptor antagonist, in the treatment of pruritus in internal and dermatological diseases. J Am Acad Dermatol 1999; 41: 533–9.
Mishra SK, Hoon MA. The cells and circuitry for itch responses in mice. Science 2013; 340: 968–71.
Monroe EW. Efficacy and safety of nalmefene in patients with severe pruritus caused by chronic urticaria and atopic dermatitis. J Am Acad Dermatol 1989; 21: 135–6.
Moser HR, Giesler GJ. Jr., Itch and analgesia resulting from intrathecal application of morphine: contrasting effects on different populations of trigeminothalamic tract neurons. J Neurosci 2013; 33: 6093–101.
Mu D, Deng J, Liu KF, Wu ZY, Shi YF, Guo WM, et al. A central neural circuit for itch sensation. Science 2017; 357: 695–9.
Nockemann D, Rouault M, Labuz D, Hublitz P, McKnelly K, Reis FC, et al. The K(+) channel GIRK2 is both necessary and sufficient for peripheral opioid-mediated analgesia. EMBO Mol Med 2013; 5: 1263–77.
North RA, Williams JT. On the potassium conductance increased by opioids in rat locus coeruleus neurones. J Physiol 1985; 364: 265–80.

Pan H, Fatima M, Li A, Lee H, Cai W, Horwitz L, et al. Identification of a spinal circuit for mechanical and persistent spontaneous itch. Neuron 2019; 103: 1135–49 e6.

Pavlis J, Yosipovitch G. Management of itch in atopic dermatitis. Am J Clin Dermatol 2018; 19: 319–32.

Peer G, Kivity S, Agami O, Fireman E, Silverberg D, Blum M, et al. Randomised crossover trial of naltrexone in uraemic pruritus. Lancet 1996; 348: 1552–4.

Qu L, Fan N, Ma C, Wang T, Han L, Fu K, et al. Enhanced excitability of MRGPRA3- and MRGPRD-positive nociceptors in a model of inflammatory itch and pain. Brain 2014; 137: 1039–50.

Reich A, Szepietowski JC. Opioid-induced pruritus: an update. Clin Exp Dermatol 2010; 35: 2–6.

Reszke R, Szepietowski JC. End-stage renal disease chronic itch and its management. Dermatol Clin 2018; 36: 277–92.

Ross SE, Mardinly AR, McCord AE, Zurawski J, Cohen S, Jung C, et al. Loss of inhibitory interneurons in the dorsal spinal cord and elevated itch in Bhlhb5 mutant mice. Neuron 2010; 65: 886–98.

Ruan X, Bumgarner GW, Kaye AD. Species variation in effects of intrathecal kappa-opioid receptor agonist on morphine-induced itch and antinociception. Reg Anesth Pain Med 2016; 41: 414.

Sakakihara M, Imamachi N, Saito Y. Effects of intrathecal kappa-opioid receptor agonist on morphine-induced itch and antinociception in mice. Reg Anesth Pain Med 2016; 41: 69–74.

Serrano L, Martinez-Escala ME, Zhou XA, Guitart J. Pruritus in cutaneous T-cell lymphoma and its management. Dermatol Clin 2018; 36: 245–58.

Singh R, Patel P, Thakker M, Sharma P, Barnes M, Montana S. Naloxone and maintenance naltrexone as novel and effective therapies for immunotherapy-induced pruritus: a case report and brief literature review. J Oncol Pract 2019; 15: 347–8.

Sun S, Xu Q, Guo C, Guan Y, Liu Q, Dong X. Leaky gate model: intensity-dependent coding of pain and itch in the spinal cord. Neuron 2017; 93: 840–53 e5.

Sun YG, Chen ZF. A gastrin-releasing peptide receptor mediates the itch sensation in the spinal cord. Nature 2007; 448: 700–3.

Sun YG, Zhao ZQ, Meng XL, Yin J, Liu XY, Chen ZF. Cellular basis of itch sensation. Science 2009; 325: 1531–4.

Tejada MA, Montilla-Garcia A, Cronin SJ, Cikes D, Sanchez-Fernandez C, Gonzalez-Cano R, et al. Sigma-1 receptors control immune-driven peripheral opioid analgesia during inflammation in mice. Proc Natl Acad Sci USA 2017; 114: 8396–401.

Umeuchi H, Togashi Y, Honda T, Nakao K, Okano K, Tanaka T, et al. Involvement of central mu-opioid system in the scratching behavior in mice, and the suppression of it by the activation of kappa-opioid system. Eur J Pharmacol 2003; 477: 29–35.

Wang D, Tawfik VL, Corder G, Low SA, Francois A, Basbaum AI, et al. Functional divergence of delta and mu opioid receptor organization in CNS pain circuits. Neuron 2018; 98: 90–108 e5.

Wang X, Zhang J, Eberhart D, Urban R, Meda K, Solorzano C, et al. Excitatory superficial dorsal horn interneurons are functionally heterogeneous and required for the full behavioral expression of pain and itch. Neuron 2013; 78: 312–24.

Wang Z, Donnelly CR, Ji RR. Scratching after stroking and poking: a spinal circuit underlying mechanical itch. Neuron 2019; 103: 952–4.

Wang Z, Jiang C, He Q, Matsuda M, Han Q, Wang K, et al. Anti-PD-1 treatment impairs opioid antinociception in rodents and nonhuman primates. Sci Transl Med 2020; 12: eaaw6471.

Xu B, Zhang M, Shi X, Zhang R, Chen D, Chen Y, et al. The multifunctional peptide DN-9 produced peripherally acting antinociception in inflammatory and neuropathic pain via mu- and kappa-opioid receptors. Br J Pharmacol 2020; 177: 93–109.

Zhang XY, Dou YN, Yuan L, Li Q, Zhu YJ, Wang M, et al. Different neuronal populations mediate inflammatory pain analgesia by exogenous and endogenous opioids. Elife 2020; 9: e55289.